THE STEWARTSON LAYER UNDER THE INFLUENCE OF THE LORENTZ AND ARCHIMEDEAN FORCES

I. Cupal[1], P. Hejda[1], and M. Reshetnyak[2]

The influence of the Lorentz force on the Stewartson layer evolving at the rotating inner core is investigated for the case when its nonlinear effects are not ignored. The influence of the imposed Archimedean force is also examined. The problem is solved using a finite difference method for the basic physical variables of velocity, magnetic field, and pressure. The pressure variable is subsequently corrected by a fractional step method. When only viscous forces are assumed at the inner core boundary, no differences with the previous results are found. However, when the influence of the Lorentz force is considered and all its nonlinear effects are taken into account, the superrotation of the outer core exhibits a different character and a larger amplitude than in the case when the nonlinear effects are ignored. The Archimedean force distinctly increases the Stewartson layer width and thus the change in the azimuthal velocity at the inner core boundary is not as sharp.

1. Introduction. The Stewartson layer, that evolves at the cylinder circumscribing the rotating Earth's inner core, and the Ekman layers at the core-mantle boundary (CMB) and at the inner core boundary (ICB) complicate the problem on numerical simulation of the geodynamo. These layers are caused by the fluid viscosity and may be very thin when the viscosity is sufficiently small. Such thin layers usually create many difficulties for any numerical process applied to solve the dynamo equation. This is particularly true for the Stewartson layer and, therefore, its behavior under different conditions has been examined in several studies. Hollerbach [9] assumed that the inner core and the mantle are insulators. He also considered the imposed rotation of the inner core relative to the outer core and the imposed dipole magnetic field fitted with the inner core. Hollerbach's numerical results were revised by Anufriev and Hejda [1, 2] in an inviscid approximation. The main results of their work was that an increase of the imposed magnetic field leads to the destruction of the Stewartson layer, a fact that is very suitable for the solution of the self-consistent dynamo problem. Note that otherwise we have to resolve structures with a spatial scale of order $E^{1/3}$ where the Ekman number $E < 10^{-8}$. The next step in the examination of the Stewartson layer was made in [4]. In addition to Hollerbach's assumptions [9], the authors of [4] assumed that the inner core is conductive and also took the linearized Lorentz force into account. They found an interesting effect of so-called superrotation of the outer core, where a part of the outer core rotates faster than ICB. Recall that in [4] the Stewartson layer was also analyzed in detail for the pure viscous case in which the Lorentz force is ignored. They were able to follow the Proudman [10] asymptotics and to confirm some conclusions made in [11].

No previous studies examined the influence of the nonlinear terms in the Lorentz force on the Stewartson layer or the influence of the Archimedean force. This paper is an attempt to investigate these influences and, at the same time, to try another numerical method. Namely, the previous studies mostly used the decomposition into spherical harmonics (spectral methods). In this paper a grid method of discretization is applied instead of the spectral method where the pressure is eliminated. We solve the equations in basic physical variables and use a fractional step method for pressure correction to provide the divergence of velocity [5, 3, 8]. The numerical method is also tried in the pure viscous case in which the Archimedean and Lorentz forces are ignored. However, we do not repeat the detailed study presented in [4], where the Ekman number was decreased down to $E = 10^{-8}$ and the conclusion that for $E < 10^{-4}$ the Proudman asymptotics started to be visible was obtained. Nevertheless, a comparison of our solution in the pure viscous case with [4] and [9] is possible. In addition, the solution with neglected nonlinear terms in the Lorentz force can be compared with that given in [4].

2. Basic equations and the numerical method. Let the outer spherical boundary of the liquid outer core of radius r_0 rotate with an angular velocity Ω (the Earth's rotation rate). Let the inner core of radius r_i rotate with a prescribed angular velocity $\Omega + \omega_i$. This means that ω_i is the prescribed rotation of the inner

[1] Geophysical Institute, Acad. Sci, 141 31 Prague, Czech Republic; e-mail: ph@ig.cas.cz
[2] United Institute of the Physics of the Earth, Russian Acad. Sci, 123995, Moscow, Russian Federation; e-mail: maxim@uipe-ras.scgis.ru; Research Computing Center of Moscow State University, 119992, Moscow, Russian Federation; e-mail: reshet@srcc.msu.su

core relative to CMB. Accepting $L = r_0$ as the length scale and L^2/η as the time scale, we scale the velocity $\mathbf{v}$, the magnetic field $\mathbf{B}$, and the pressure p as η/L, $\sqrt{2\Omega\rho\mu\eta}$, and $2\Omega\rho\eta$, respectively. Here ρ is an average density of the core, μ its permeability, and η the diffusivity of the outer core. In the magnetic case we will assume the imposed dipole field $\mathbf{B_0}$ in the outer core to be fitted with the rotating ICB. Inside the inner core this dipole field is assumed to be zero. Therefore, the magnetic field is $\mathbf{B}_0 + \mathbf{b}$ in the outer core and $\mathbf{b}$ in the inner core, where $\mathbf{b}$ is the induced magnetic field. The induction equation and the equation of motion describing the problem in the outer core are

$$R_0 \left(\frac{\partial \mathbf{v}}{\partial t} + \mathbf{v} \cdot \nabla \mathbf{v} \right) = -\nabla p + \mathbf{F} + E \nabla^2 \mathbf{v}, \qquad (2.1)$$

$$\frac{\partial \mathbf{b}}{\partial t} = \nabla \times \big(\mathbf{v} \times (\mathbf{B_0} + \mathbf{b}) \big) + \nabla^2 \mathbf{b}. \qquad (2.2)$$

In the inner core the induction equation can be reduced to

$$\frac{\partial \mathbf{b}}{\partial t} = \nabla \times (r_i \omega_i \sin \theta \, \mathbf{1}_\varphi \times \mathbf{b}) + \nabla^2 \mathbf{b}. \qquad (2.3)$$

Moreover, in the outer and inner cores the equations

$$\nabla \cdot \mathbf{v} = 0, \qquad \nabla \cdot \mathbf{b} = 0 \qquad (2.4)$$

can be solved. The sum of the Archimedean ($\mathbf{F}_a$), Coriolis, and Lorentz ($\mathbf{F}_L$) forces in the outer core is represented as

$$\mathbf{F} = \mathbf{F}_a - (\mathbf{1}_z \times \mathbf{v}) + \mathbf{F}_L, \qquad (2.5)$$

where for the imposed dipole magnetic field the Lorentz force is

$$\mathbf{F}_L = (\nabla \times \mathbf{b}) \times \mathbf{B}_0 + (\nabla \times \mathbf{b}) \times \mathbf{b}. \qquad (2.6)$$

The Ekman number and the Rossby number appear in the equations:

$$E = \frac{\nu}{2\Omega L^2}, \qquad R_0 = \frac{\eta}{2\Omega L}.$$

The equations are accompanied by the boundary conditions

$$v_r = v_\theta = 0, \quad v_\varphi = r_i \omega_i \sin \theta, \quad \mathbf{b} \text{ continuous at ICB,}$$

$$v_r = v_\theta = v_\varphi = 0, \quad \mathbf{b} \text{ potential at CMB.} \qquad (2.7)$$

In the practical calculation the inertial terms in the left-hand side of (2.1) can be ignored, since R_0 is chosen sufficiently small. However, we temporarily leave the time derivative $\partial \mathbf{v}/\partial t$ in its place at the beginning of the numerical process to keep the parabolic structure of PDE and integrate the equations up to a stable steady-state where this derivative becomes negligible.

The numerical method in use is described in [6, 7, 8] in sufficient detail. Therefore, only the main features of our approach will be outlined here. The transformed variables $f = r^{-1}F$ are used instead of the components of velocity, magnetic field, and pressure to avoid singularity of the magnetic field at the center. Thus, the zero boundary conditions at the center can be applied for all variables. The system (2.1)–(2.6) then leads to a system of linear algebraic equations due to the nonstaggered grid in the r- and θ-directions. The second order terms are treated implicitly using the Gauss–Seidel scheme to avoid Courant's problem for small time steps. Having b_θ and b_φ from (2.2) or (2.3), the b_r-component is obtained from the second equation (2.4). Actually, this equation is only a restriction in the initial condition for the magnetic field in the induction equation. However, that is not the case for the velocity in (2.1). The solution of this equation requires an additional equation for pressure.

The problem of how to satisfy the first equation (2.4) can then be solved using spatial time splitting (a fractional step method) as used, for instance, in [5] or [3] (see also [8]). In principle, the steady-state solution is obtained by successive integration of the parabolic problem (2.1) (the convective term in the left-hand side is omitted), where the velocity v is split into two parts at each time step n: $\mathbf{v}^n = \mathbf{U}^n + \mathbf{u}^n$ having $\nabla \cdot \mathbf{v}^n = 0$. At the next time step, the equation is first solved without the pressure term

$$R_0 \frac{\mathbf{U}^{n+1} - \mathbf{v}^n}{\delta t} = \mathbf{F}^n + E \nabla^2 \mathbf{v}^n$$

with the boundary conditions $R_0 U_\tau^{n+1} = \delta t\, \partial p^n/\partial \tau + v_\tau^{\mathrm{ICMB}}$ and $U_r^{n+1} = 0$ at ICB and CMB. Here τ indicates the tangential components ($\tau = \theta,\ \varphi$) and the derivatives ($\partial/\partial \tau = \partial/r\, \partial\theta,\ \partial/r\sin\theta\, \partial\varphi$), whereas v_τ^{ICMB} represents the boundary condition for the tangential velocity components (2.7) at ICB and CMB. The correction of velocity is then computed with the help of the pressure variable. Applying the divergence $\nabla\cdot$ to equation (2.1), we get the Poisson equation

$$\nabla^2 p^{n+1} = \nabla\cdot\left(\mathbf{F}^n + E\nabla^2\mathbf{v}^n\right) = \frac{R_0}{\delta t}\nabla\cdot\mathbf{U}^{n+1},$$

which is solved with the boundary condition $\partial p^{n+1}/\partial r = 0$ at ICB and CMB. The correction of velocity is then $R_0\mathbf{u}^{n+1} = -\delta t\,\nabla p^{n+1}$. Therefore, $\mathbf{v}^{n+1}$ satisfies (2.1) and the first equation (2.4). At the same time, the boundary condition for the radial velocity component at ICB and CMB are satisfied.

3. Numerical results and discussion. In all calculations we assume $r_0 = 1$, $r_i = 0.4$, and $R_0 = E$. The stabilized steady-state solution was found in all cases and, therefore, the role of the Rossby number is marginal.

The first step in our calculations was directed to obtain the Stewartson layer without any external force. Therefore, $\mathbf{F}_a$ and $\mathbf{F}_L$ in (2.5) are omitted. The prescribed $\omega_i = 1$ was considered and the model was calculated for the Ekman numbers $E = 10^{-3},\ 3\cdot 10^{-4},\ 10^{-4}$. Figure 1 shows the expected dependence of the Stewartson layer thickness on the decreasing Ekman number. The behavior of the Stewartson layer in the above cases is the same as in the previous investigation in [4]; this allows us to state that our numerical approach is suitable for this task. It is not a purpose of this paper to confirm the Proudman asymptotic solution [10], which can be followed for smaller Ekman numbers.
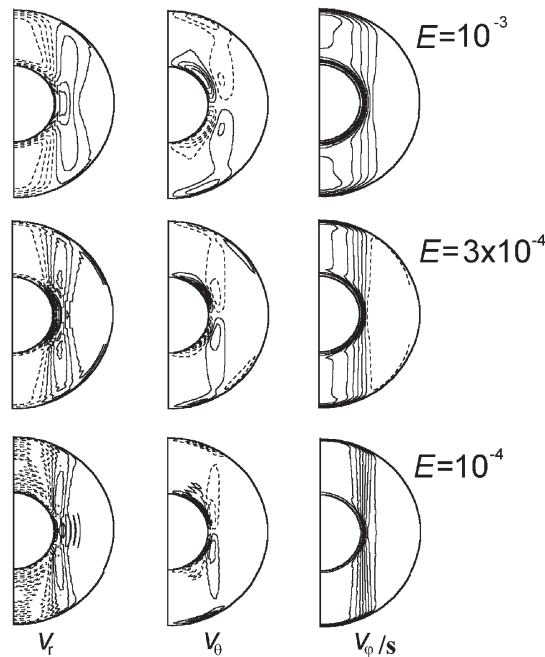

Fig. 1. Meridional sections of the velocity components in the pure viscous case for the Ekman numbers
$E = 10^{-3}$, $E = 3\cdot 10^{-4}$, and $E = 10^{-4}$

The dependence of the Stewartson layer thickness on an amplitude of the Archimedean force was also investigated. The Lorentz force F_L in (2.5) was omitted and $\omega_i = 1$ was again considered. The Archimedean force was prescribed only radially dependent

$$\mathbf{F}_a = F_a(r_0 - r)(r - r_i)\,\mathbf{1}_r.$$

Our calculations were made for $E = 3\cdot 10^{-4}$ and $F_a = 0.3,\ 3.0$. Figure 2 shows the influence of the Archimedean force amplitude on the Stewartson layer thickness. The thickness increases as the Archimedean force amplitude increases.

The dependence of the Stewartson layer on the Lorentz force was observed without the presence of any Archimedean force ($\mathbf{F_a} = 0$). For this purpose, the imposed dipole field is assumed in the outer core to be fitted
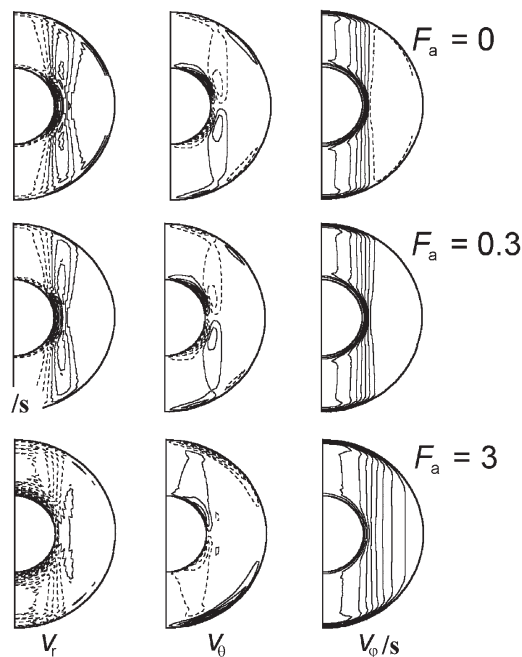
Fig. 2. Meridional sections of the velocity component when the prescribed Archimedean force is applied and the Ekman number $E = 3 \cdot 10^{-4}$ is considered

with the rotating ICB:

$$\mathbf{B}_0 = \frac{r_i^3 B_0}{3r^3} \left(2\,\mathbf{1}_r \cos\theta + \mathbf{1}_\theta \sin\theta \right).$$

In this case the prescribed rotation of the inner core is considered $\omega_i = 0.1$ and the Ekman number was again taken $E = 3 \cdot 10^{-4}$. We considered values $B_0 = 4.8, 5.4, 35.8, 44.8$.

In the linearized case, the second term in the right-hand side of (2.6) is omitted. This case should relate to the similar investigation in [4]. The superrotation is also observed in the equatorial region (see Figure 3) with the maximum of the azimuthal velocity shifting away from ICB with the increasing amplitude of the imposed dipole field.

Except in the case of $B_0 = 4.8$, the amplitude of the superrotation of the outer core does not change with the increasing amplitude of the imposed dipole. This result is also in agreement with findings in [4], although the authors of [4] observed a slow depression of the amplitude of superrotation for large amplitudes of the imposed dipole. Nevertheless, in the range of amplitudes $B_0 \in (5.4, 44.8)$ we considered, they also observed no change in the amplitude of superrotation. Figure 4 demonstrates that the typical cylindrical structure of the Stewartson layer is destroyed.

When the second term in the right-hand side of (2.6) is included, the nonlinear effects of the Lorentz force slightly change the picture that can be observed in the linearized case. The typical cylindrical structure of the Stewartson layer is again destroyed; however, this destruction is stronger (see Figure 5).

Calculating the nonlinear case for the same values as the previous linear one, we can again observe super-rotation with the maximum of the azimuthal velocity shifting away from ICB. However, it is essential that its amplitude increases when the imposed dipole amplitude increases (see Figure 6). This effect was not observed in the linearized case. Moreover, the amplitude of superrotation is two or three times larger than that in the linearized case. Therefore, the nonlinear terms in the Lorentz force play an important role in influencing the velocity in the outer core.

4. Conclusion. The Stewartson layer appeared in the pure viscous case when the Archimedean and Lorentz forces are omitted ($F_a = 0$, $B_0 = 0$). These calculations bring nothing new to the research of the Stewartson layer and only confirm previous investigations made in [9] and [4]. The Proudman asymptotics were not tested. Our calculations of the pure viscous case can be considered as a good test of our codes.

The imposed Archimedean force ($F_a \neq 0$, $B_0 = 0$) in radial direction brings new findings. The increasing amplitude of the Archimedean force leads to the increased thickness of the Stewartson layer while the cylindrical
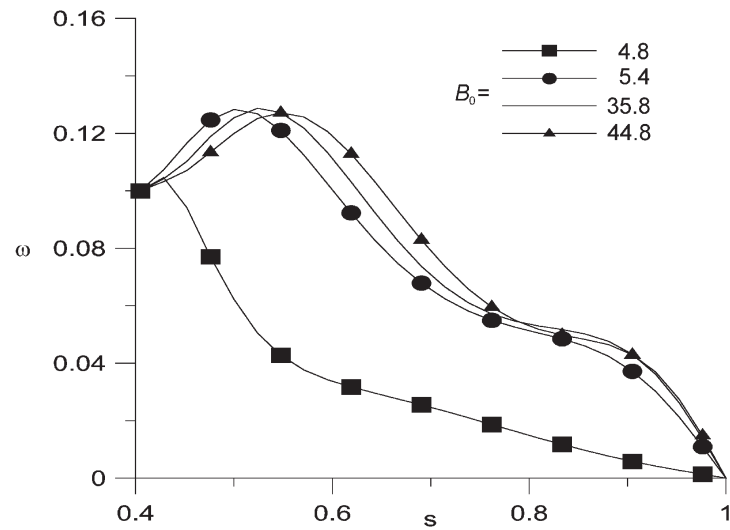
Fig. 3. Dependence of the angular velocity $\omega = v_\varphi/s$ in the equatorial plane on the cylindrical radius $s = r\sin\theta$ for different magnitudes of the imposed magnetic dipole: $B_0 = 4.8$, $B_0 = 5.4$, $B_0 = 35.8$, and $B_0 = 44.8$. The Ekman number $E = 3 \cdot 10^{-4}$ is considered and the nonlinear terms in the Lorentz force are ignored
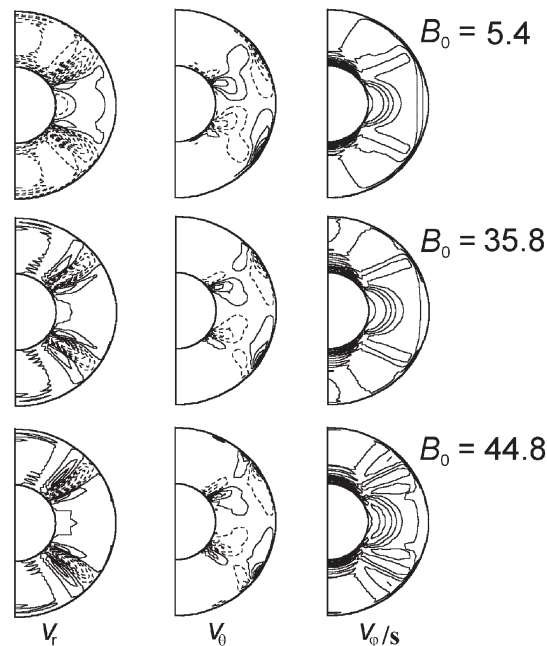

Fig. 4. Meridional sections of the velocity components when the imposed magnetic dipole is applied within the outer core: $B_0 = 5.4$, $B_0 = 35.8$, and $B_0 = 44.8$. The Ekman number $E = 3 \cdot 10^{-4}$ is considered and the nonlinear terms in the Lorentz force are ignored

character of the layer remains unchanged. Therefore, the azimuthal component of the velocity changes more slowly, crossing the cylinder circumscribing the inner core, than in the pure viscous case. A significant influence on the Ekman layers at ICB or CMB was not observed.

The imposed dipole field ($F_a = 0$, $B_0 \neq 0$) causes the generation of the magnetic field in the outer and inner cores and thus the Lorentz force influences the flow in the outer core. When only the linearized Lorentz force is considered, the effects observed in [4] are confirmed. In particular, the superrotation of the outer core appears and when the imposed dipole amplitude increases, the maximum of the azimuthal velocity shifts away from
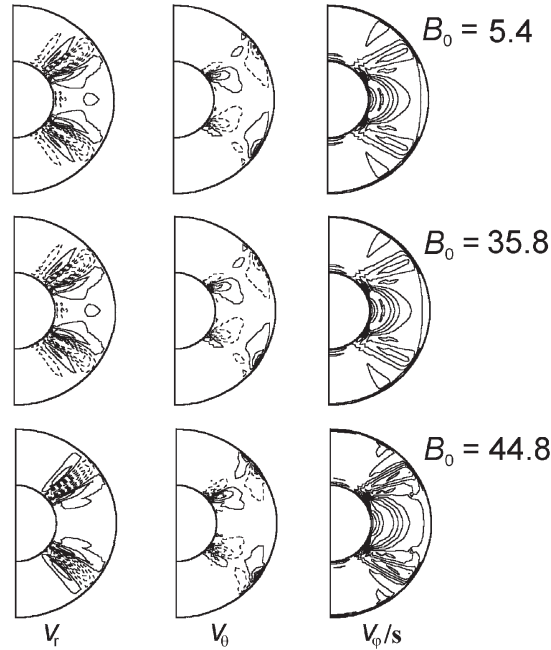
Fig. 5. Meridional sections of the velocity components when the imposed magnetic dipole is applied within the outer core: $B_0 = 5.4$, $B_0 = 35.8$, and $B_0 = 44.8$. The Ekman number $E = 3 \cdot 10^{-4}$ is considered and the nonlinear terms in the Lorentz force are taken into account
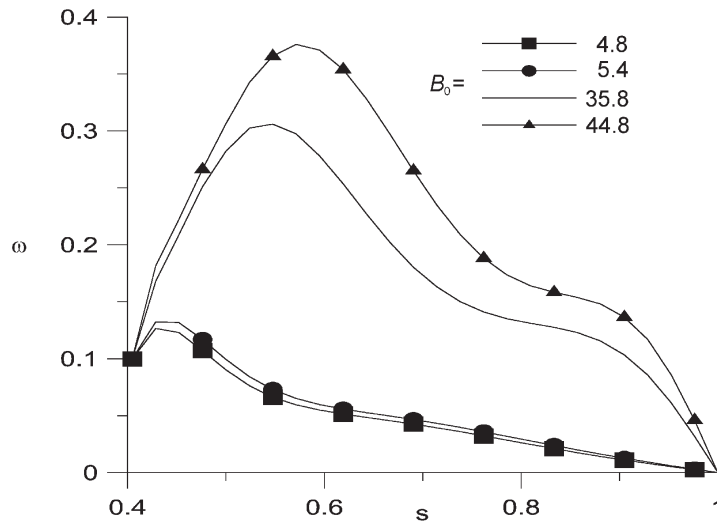

Fig. 6. Dependence of the angular velocity $\omega = v_\varphi/s$ in the equatorial plane on the cylindrical radius $s = r \sin \theta$ for the different magnitudes of the imposed magnetic dipole: $B_0 = 4.8$, $B_0 = 5.4$, $B_0 = 35.8$, and $B_0 = 44.8$. The Ekman number $E = 3 \cdot 10^{-4}$ is considered and the nonlinear terms in the Lorentz force are taken into account

ICB. At the same time, the amplitude of this superrotation remains unchanged for a relatively large interval of strength of the imposed dipole. When the nonlinear terms are also considered in the Lorentz force (this was not a subject of the study in [4]), new effects can be observed. In addition to the previous effects caused by the linearized Lorentz force, the amplitude of super-rotation increases as the imposed dipole amplitude increases. The amplitude of superrotation is also two or three times larger than that in the linearized case. The structure of the Stewartson layer is no more cylindrical in either the linearized or the nonlinear case. However, in the

nonlinear case this destruction is much stronger.

References

1. *A.P. Anufriev and P. Hejda*, "Effect of the magnetic field at the inner core boundary on the flow in the Earth's core", *Phys. Earth Planet. Int.*, **106**: 19–30, 1998.
2. *A.P. Anufriev and P. Hejda*, "The influence of a homogeneous magnetic field on the Ekman and Stewartson layers", *Studia Geoph. et Geod.*, **42**: 254–260, 1998.
3. *C. Canuto, M.Y. Hussini, A. Quarteroni, and T.A. Zang*, Spectral Methods in Fluids Dynamics, Berlin: Springer-Verlag, 1988.
4. *E. Dormy, P. Cardin, and D. Jault*, "MHD flow in a slightly differentially rotating spherical shell, with conducting inner core, in a dipolar magnetic field", *Phys. Earth Planet. Int.*, **160**: 15–30, 1998.
5. *C.J. Heinrich and D.W. Pepper*, Intermediate Finite Element Method, New York: Taylor & Francis, 1999.
6. *P. Hejda and M. Reshetnyak*, "A grid-spectral method of the solution of the 3D kinematic geodynamo with the inner core", *Studia Geoph. et. Geod.*, **43**: 319–325, 1999.
7. *P. Hejda and M. Reshetnyak*, "The grid-spectral approach to 3D geodynamo modeling", *Computers & Geosciences*, **26**: 167–175, 2000.
8. *P. Hejda, I. Cupal, and M. Reshetnyak*, "On the application of grid-spectral method to the solution of geodynamo equations", In: *Dynamo and Dynamics, a Mathematical Challenge*, ed. by P. Chossat, D. Armbruster, I. Oprea. Nato Sci. Ser., **26/II**, Dordrecht: Kluwer Acad. Publ., 181–187, 2001.
9. *R. Hollerbach*, "Magnetohydrodynamic Ekman and Stewartson layers in a rotating spherical shell", *Proc. Roy. Soc.*, **A444**: 333–346, 1994.
10. *I. Proudman*, "The almost-rigid rotation of viscous fluid between concentric spheres", *J. Fluid. Mech.*, **1**: 505–516, 1956.
11. *K. Stewartson*, "On almost-rigid rotations", *J. Fluid. Mech.*, **26**: 131–144, 1966.